Enhanced 2D-image upconversion using solid-state lasers

Pedersen, Christian; Karamehmedovic, Emir; Dam, Jeppe Seidelin; Tidemand-Lichtenberg, Peter

Published in:
Optics Express

Link to article, DOI:
10.1364/OE.17.020885

Publication date:
2009

Document Version
Publisher's PDF, also known as Version of record

Enhanced 2D-image upconversion using solid-state lasers

Christian Pedersen[1]*, Emir Karamehmedović[1], Jeppe Seidelin Dam[1] and Peter Tidemand-Lichtenberg[2]

[1]*DTU Fotonik, Technical University of Denmark, DK-4000 Roskilde, Denmark*
[2]*DTU Physics, Technical University of Denmark, DK-2800 Kgs. Lyngby, Denmark*
**christian.pedersen@risoe.dk*

Abstract: Based on enhanced upconversion, we demonstrate a highly efficient method for converting a full image from one part of the electromagnetic spectrum into a new desired wavelength region. By illuminating a metal transmission mask with a 765 nm Gaussian beam to create an image and subsequently focusing the image inside a nonlinear PPKTP crystal located in the high intra-cavity field of a 1342 nm solid-state Nd:YVO_4 laser, an upconverted image at 488 nm is generated. We have experimentally achieved an upconversion efficiency of 40% under CW conditions. The proposed technique can be further adapted for high efficiency mid-infrared image upconversion where direct and fast detection is difficult or impossible to perform with existing detector technologies.

OCIS codes: (140.3480) Lasers, diode-pumped; (140.3580) Lasers, solid-state; (140.7300) Visible lasers; (190.7220) Upconversion; (110.3080) Infrared imaging.

References and Links

1. R. A. Andrews, "Wide angular aperture image up-conversion," J. Quantum Electron. **5**(11), 548–550 (1969).
2. A. H. Firester, "Image upconversion: Part III*," J. Appl. Phys. **41**(2), 703–709 (1970).
3. W. Chiou, "Geometric Optics Theory of Parametric Image Upconversion," J. Appl. Phys. **42**(5), 1985–1993 (1971).
4. J. Falk, and Y. C. See, "Internal CW parametric upconversion," Appl. Phys. Lett. **32**(2), 100–101 (1978).
5. J. E. Midwinter, "Infrared up conversion in lithium-niobate with large bandwidth and solid acceptance angle," Appl. Phys. Lett. **14**(1), 29–32 (1969).
6. S. Guha, and J. Falk, "The effects of focusing in the three-frequency parametric up converter," J. Appl. Phys. **51**(1), 50–60 (1980).
7. F. Devaux, A. Mosset, E. Lantz, S. Monneret, and H. Le Gall, "Image upconversion from the visible to the UV domain: application to dynamic UV microstereolithography," Appl. Opt. **40**(28), 4953–4957 (2001), http://www.opticsinfobase.org/ao/abstract.cfm?URI=ao-40-28-4953.
8. E. Karamehmedović, C. Pedersen, M. T. Andersen, and P. Tidemand-Lichtenberg, "Efficient visible light generation by mixing of a solid-state laser and a tapered diode laser," Opt. Express **15**(19), 12240–12245 (2007), http://www.opticsinfobase.org/abstract.cfm?id=141313.
9. E. Karamehmedović, C. Pedersen, O. B. Jensen, and P. Tidemand-Lichtenberg, "Nonlinear beam clean-up using resonantly enhanced sum-frequency mixing," Appl. Phys. B **96**(2-3), 409–413 (2009).
10. D. J. Stothard, M. H. Dunn, and C. F. Rae, "Hyperspectral imaging of gases with a continuous-wave pump-enhanced optical parametric oscillator," Opt. Express **12**(5), 947–955 (2004), http://www.opticsinfobase.org/oe/abstract.cfm?URI=oe-12-5-947.
11. J. W. Goodman, "Introduction to Fourier Optics" (Third edition), Robers & Company Publishers (2005).
12. G. D. Boyd, and D. A. Kleinman, "Parametric Interaction of Focused Gaussian Light beams," J. Appl. Phys. **39**(8), 3597–3640 (1968).

1. Introduction

An efficient way to transform light from one part of the spectrum into another, desired part is by using intra-cavity upconversion. Upconversion has been investigated for decades but with a particularly strong focus in the late 1960s to mid 1980s [1–7]. However, one important parameter limiting the applications of the upconversion process has been the upconversion efficiency. Efficient upconversion is important especially for applications requiring high sensitivity and can even be traded for increased resolution in the image formation. One

#116265 - $15.00 USD Received 26 Aug 2009; revised 28 Oct 2009; accepted 28 Oct 2009; published 30 Oct 2009

method to enhance the efficiency has been intra-cavity upconversion. This was first demonstrated using lasers [4], but the efficiency was here limited by the intra-cavity loss originating from absorption in the nonlinear crystal. The (non-imaging) upconversion efficiency was reported to be 0.38% at best. During the last thirty years only a tiny fraction of reported upconversion work has involved imaging.

Using a diode-pumped, high finesse, solid-state laser at 1342 nm and a tapered diode laser at 765 nm, more than 300 mW of upconverted 488 nm light was generated in a periodically-poled $KTiOPO_4$ (PPKTP) crystal. The power conversion efficiency from 765 nm to 488 nm was 32% [8]. It has also been shown that a non-Gaussian tapered diode laser beam can be spatially filtered using SFG with a Gaussian solid-state laser beam to produce a SFG beam with a nearly Gaussian profile [9]. The spatial filter characteristics depend on the spatial overlap in the focus plane of the two interacting beams. If the Fourier transform of a non-Gaussian tapered diode beam is focused to a size where only its fundamental Gaussian spatial component overlaps the Gaussian beam of the solid-state laser, it is possible to obtain a nearly Gaussian SFG beam. Similarly, if strong focusing is utilized, all the detailed spatial features of the tapered diode laser beam appear in the SFG beam.

If the input beam comprises several spatial frequencies originating from a coherently illuminated object, i.e. not necessarily a near Gaussian field distribution, in this paper it will be demonstrated that it is possible to transform the object field at one wavelength into a new wavelength, with high conversion efficiency. A special aspect of the reported method is that it is all optical and performs an upconversion of a full 2-dimensional image. This is in contrast to the more conventional method based on upconverting one point at a time in combination with a x,y-scanning device [10], thus gaining in simplicity and speed.

2. Theory

In the following, an expression for the intensity profile of an upconverted object field, $E_{object} = E_{object}(x,y)$ will be derived, where x and y denote the transverse coordinates of the field. The upconverted image, $E_{up} = E_{up}(x,y)$, is the result of the upconversion process between E_{object} and a Gaussian intra-cavity field, $U_{Gauss} = U_{Gauss}(u,v)$, where u and v are the transverse coordinates at the Fourier plane. The specific system under consideration is shown in Fig. 1.

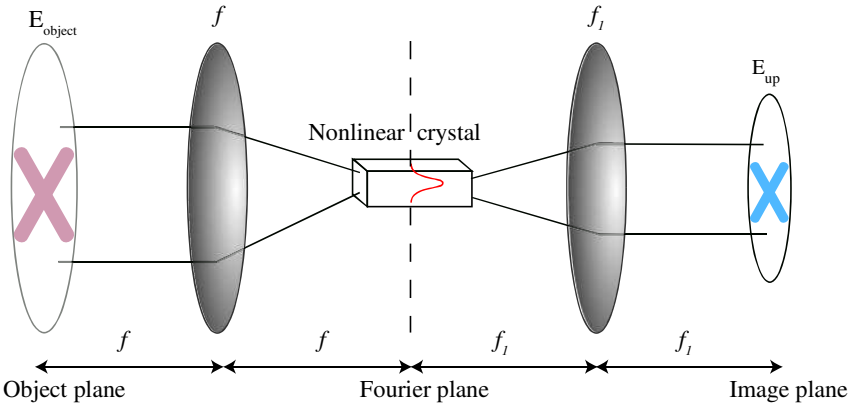

Fig. 1. The system under consideration; An object field is focussed to the Fourier plane inside a nonlinear crystal where it interacts with the Gaussian intra-cavity field of a diode-pumped solid-state laser to generate an upconverted field at the image plane.

It is assumed that the object field is subject to coherent monochromatic illumination [11]. For simplicity, it is further assumed that the system is operated in the non-saturated regime. This assumption implies that the amplitudes of the generating fields, E_{object} and U_{Gauss} can be approximated as being constant throughout the entire interaction length of the nonlinear crystal. Further, a plane wave approximation is used, and finally, the length of the crystal is considered to be short compared to the confocal length of the interacting beams. All these

#116265 - $15.00 USD Received 26 Aug 2009; revised 28 Oct 2009; accepted 28 Oct 2009; published 30 Oct 2009

assumptions are not strictly necessary, but allow derivation of a simple relation between the light from the object and the corresponding upconverted image at the image plane. Using the mentioned assumptions, E_{up} can be calculated as:

$$E_{up}(x,y) = j\frac{2\pi d_{eff} L\lambda_1 f}{n_3 f_1 \lambda_3^2 w_0}\sqrt{\frac{4P_{Gauss}}{\pi n_2 \varepsilon_0 c}}E_{object}\left(-\frac{\lambda_1 f}{\lambda_3 f_1}x,-\frac{\lambda_1 f}{\lambda_3 f_1}y\right)\otimes\left(\frac{\pi w_0^2}{\lambda_3^2 f_1^2}e^{-\frac{x^2+y^2}{\left(\frac{\lambda_3 f_1}{\pi w_0}\right)^2}}\right) \quad (1)$$

The upconverted wavelength λ_3 is determined by the energy conservation law: $\frac{1}{\lambda_3}=\frac{1}{\lambda_1}+\frac{1}{\lambda_2}$, where λ_2 is the wavelength of the intra-cavity Gaussian beam and λ_1 is the wavelength of light emitted from the object. n_1, n_2 and n_3 are the refractive indices of the nonlinear crystal corresponding to λ_1, λ_2 and λ_3. f and f_1 are the focal lengths of the Fourier transforming lenses, P_{Gauss} is the power of the intra-cavity Gaussian field, ε_0 is the vacuum permeability, c is the speed of light in vacuum, w_0 is the radius of the intra-cavity beam at the beam waist, d_{eff} is the effective second order nonlinearity of the crystal and L is the length of the crystal. From Eq. (1), the intensity profile of the upconverted light I_{up} can be calculated as:

$$I_{up}(x,y) = \frac{8\pi d_{eff}^2 f^2 \lambda_1^2 L^2}{n_2 n_3 f_1^2 \lambda_3^4 w_0^2}P_{Gauss}\left|E_{object}\left(-\frac{\lambda_1 f}{\lambda_3 f_1}x,-\frac{\lambda_1 f}{\lambda_3 f_1}y\right)\otimes\left(\frac{\pi w_0^2}{\lambda_3^2 f_1^2}e^{-\frac{x^2+y^2}{\left(\frac{\lambda_3 f_1}{\pi w_0}\right)^2}}\right)\right|^2 \quad (2)$$

Equation (2) shows that a spatial filtering between the object field and the Gaussian field is taking place. We note that this expression is a generalization of the usual nonlinear theory [12], where two Gaussian beams interact. In the limit where the beam radius w_0 of the intra-cavity Gaussian field becomes sufficiently large (effectively transforming the normalized convolution function into a delta-function), a perfect upconverted replica of the original image, in the new spectral region can be obtained, scaled with a factor $-\frac{\lambda_3 f_1}{\lambda_1 f}$.

$$I_{up}(x,y) = \frac{16\pi d_{eff}^2 f^2 \lambda_1^2 L^2}{n_1 n_2 n_3 c\varepsilon_0 f_1^2 \lambda_3^4 w_0^2}P_{Gauss}I_{object}\left(-\frac{\lambda_1 f}{\lambda_3 f_1}x,-\frac{\lambda_1 f}{\lambda_3 f_1}y\right) \quad (3)$$

Equation (3) is the main result of the analysis. It is noted that the point spread function $P(x,y,x_0,y_0)$ can be expressed as:

$$P(x,y,x_0,y_0) = j\frac{2\pi^2 d_{eff} L w_0}{n_3 f \lambda_1 f_1 \lambda_3^2}\sqrt{\frac{4P_{Gauss}}{\pi n_2 \varepsilon_0 c}}e^{-\frac{(x-x_0)^2+(y-y_0)^2}{\left(\frac{\lambda_3 f_1}{\pi w_0}\right)^2}} \quad (4)$$

Equation (4) is derived assuming that E_{object} is a delta function positioned at the coordinates (x_0,y_0). From Eq. (4), it can be seen that the size of the Gaussian beam defines the shape of the point spread function, and thus the resolution of the imaging process. The cost of increasing the beam size to improve the resolution is a reduced intensity (assuming constant power), therefore the conversion efficiency reduces accordingly. However, another important and limiting parameter in the image upconversion is the acceptance bandwidth of the nonlinear process. The angular acceptance parameter of the SFG process acts as a filter limiting the maximum size of E_{object} to be converted. Similarly, the spectral acceptance parameter defines the spectral width of frequencies that can be upconverted in a specific set-up.

#116265 - $15.00 USD Received 26 Aug 2009; revised 28 Oct 2009; accepted 28 Oct 2009; published 30 Oct 2009

3. Setup

The setup used in the experiment is shown in Fig. 2. It consists of a single-frequency 765 nm external-cavity tapered diode laser (ECDL), a high finesse, Z-shaped 1342 nm solid-state laser cavity and an intra-cavity PPKTP crystal. Detailed characteristics of the 1342 nm laser can be found in [8,9]. The beam waist of the 1342 nm laser field inside the PPKTP crystal, is located approximately 60 mm from mirror M2. The size of the beam waist is 44 μm, ignoring a slight astigmatism arising from the tilted mirrors M2 and M3, as well as from the passage of Brewster cut PPKTP surfaces.

The intra-cavity power of the 1342 nm laser is measured to be approximately 120 W when the laser crystal (LC) is pumped with 2 W of 808 nm light.

The 765 nm tapered diode laser is coupled to a single-mode polarization maintaining fiber. The Gaussian output beam from the fiber is collimated by a lens L1 (f = 50 mm) to a beam diameter of approximately 10 mm. This beam is used for coherent illumination of a transmission mask [see Fig. 3(a)] to form an object beam (E_{object}). The two slits forming the cross are 1 mm by 5 mm in width. (Some minor diffraction effects appear in the transmitted image). The 765 nm object is transformed by a lens L2 (f = 100 mm) in combination with curved mirror M2 (f = –200 mm) to the Fourier plane inside the PPKTP crystal. The PPKTP crystal is placed at the beam waist in the 1342 nm cavity.

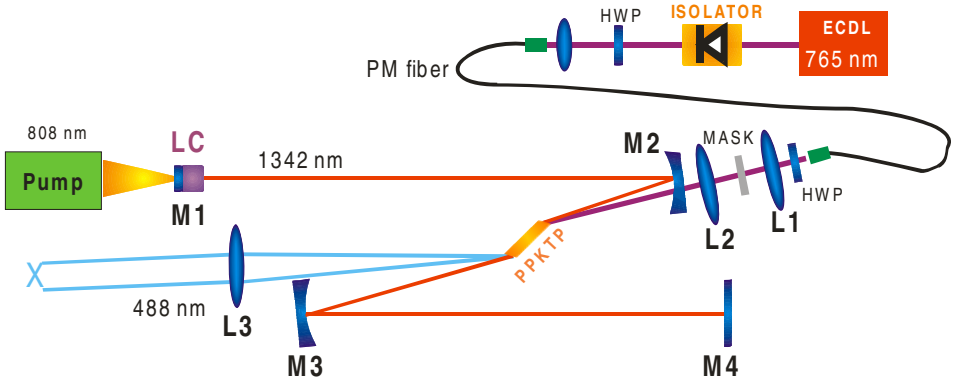

Fig. 2. Schematic of the experimental setup. The 765 nm beam from a ECDL is masked and single-passed through a PPKTP crystal placed in the beam-waist of a high-finesse 1342 nm laser for efficient SFG of the image into the blue spectral region.

The 10 mm long Brewster cut PPKTP crystal is temperature controlled using a Peltier element. The temperature is set to 43.5°C to facilitate optimum quasi-phase matching for sum frequency generation between the 1342 nm beam and the object field at 765 nm. Finally, the upconverted object field is collimated by a lens L3 (f = 75 mm) to form an upconverted image at 488 nm.

4. Results

Figure 3(a) shows the transmission mask which is coherently illuminated by the collimated 765 nm external-cavity laser. The transmitted light, after passage through the mask, corresponds to E_{object} and is shown in Fig. 3(b). The Fourier transform of the object field (E_{object}) is performed using the lens L2 (f = 100 mm) placed 80 mm from the object plane and 62 mm from mirror M2 (acting as a negative lens with f = –200 mm). At the position of the beam waist inside the PPKTP crystal, the high intra-cavity field of the 1342 nm laser and the Fourier transformed object field interact through SFG to generate a blue, 488 nm upconverted image. This is shown in Fig. 3(d). Figure 3(c) shows the calculated upconverted image using the simple theory outlined in section 2 with some additional stretching (18% on the horizontal axis and 3% on the vertical axis) originating from imaging/upconverting through the Brewster cut surfaces. The additional stretching along the horizontal axis from Brewster-cut surfaces

#116265 - $15.00 USD Received 26 Aug 2009; revised 28 Oct 2009; accepted 28 Oct 2009; published 30 Oct 2009

can be calculated to be $\cos(\theta_{765nm})/\cos(\theta_{488nm})$ where θ_λ is the incidence angle required to obtain parallel beams inside the crystal with the 1342 nm beam. For the vertical axis a careful analysis gives an additional stretching of $\sin(\theta_{488nm})/\sin(\theta_{765nm}) = n_3/n_1$ also originating from the Brewster-cut surfaces.

Comparing the measured and calculated intensity profiles, a reasonably good qualitative as well as quantitative agreement is found. Note that the effect of the point spread function smearing out the edges of the image is clearly seen.

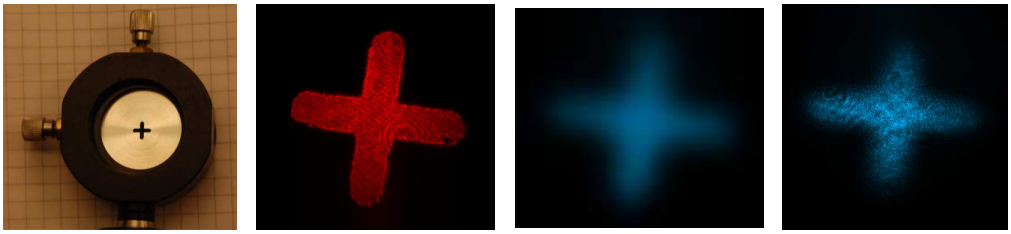

Fig. 3. (a) Transmission mask positioned at the object plane. (b) Direct image of the 765 nm coherently illuminated mask. (c) Theoretically calculated 488 nm light distribution at image plane (based on image b). (d) Measured 488 nm upconverted cross at the image plane. Images (b)-(d) have been colored to reflect the color of the light creating the patterns.

The power transmitted through the mask was measured to 15 mW, and the blue image contained 6 mW of power. Thus, a 40% power conversion efficiency, corresponding to more than 25% quantum efficiency in the image upconversion process, has been obtained. To the authors best knowledge, this is the highest upconversion efficiency of real 2-D images reported under CW condition. A power conversion efficiency of 40% corresponds to an average decrease in E_{object} of 14%. Therefore, the underlying assumption of having constant E_{object} throughout the crystal is reasonable, even at this very high conversion efficiency.

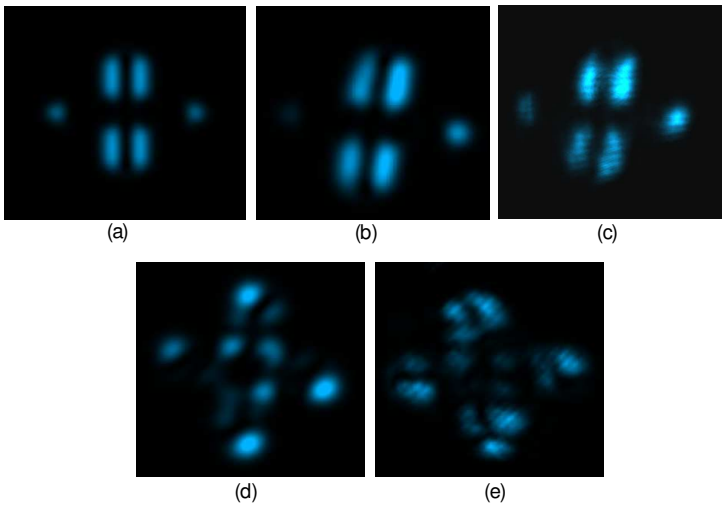

Fig. 4. Theoretical and experimental examples of offset beams inside the non-linear crystal. (a) Theoretical upconverted image arising from a beam displacement of 83 μm (1.9 w_0) along x-axis (idealized crosshair). (b) Same as (a) but calculated from Fig. 3(b). (c) Experimentally obtained upconverted image corresponding to image (b). (d) Calculation of the upconverted beam with displacement along the x-y axes based on Fig. 3(b). (e) Experimentally obtained upconverted image corresponding to image (d).

To further investigate the predictive capability of the theory, the Fourier transform of the object field [Fig. 3(b)] was translated with respect to the Gaussian field along the x- and x-y

#116265 - $15.00 USD Received 26 Aug 2009; revised 28 Oct 2009; accepted 28 Oct 2009; published 30 Oct 2009

axes, respectively. Figures 4(a)-4(c) demonstrate that a misalignment of the transverse position of the Gaussian 1342 nm beam favors the higher spatial frequency components of the object, as expected from Fourier optics theory [11].

The experimentally upconverted image is in good qualitative agreement with the theoretically predicted upconverted image.

Similarly, Figs. 4(d)-4(e) show a more complicated example where the translation has been made in the *x*-*y* plane. Also here we note a good correspondence between the predicted and measured results.

5. Discussion

The upconverted image in Fig. 3(d) is not sharp due to different types of distortion. The concave mirror M2 acts as a negative lens and induces astigmatism in the single-pass 765 nm beam due to the oblique angle of incidence. This source of distortion can be removed using a resonator geometry where the object beam is transmitted through a plane mirror. Another distorting effect is the spatial filtering relating to the point spread function. The 1342 nm beam has a Gaussian profile and upconverts the high-frequency components of the image with lower efficiency than the low-frequency components. Thus, the upconverted image has no sharp edges. A larger 1342 nm beam profile or stronger focusing of the infrared image would improve the quality (resolution) of the upconverted image. However, increasing the diameter of the 1342 nm beam decreases the conversion efficiency, while stronger focusing is limited by the angular acceptance parameter of the nonlinear crystal, i.e. the effective size of the object E_{object} that can be converted is reduced. Thus, a trade-off is encountered, allowing for optimization of one of the two parameters only at the expense of the other.

An approximate value for the maximum resolution, of the current setup can be estimated to be 10x10 pixels. This can however be upgraded easily either by using a shorter crystal, allowing for larger angles, or by redesigning the laser cavity to support a larger beam diameter. While the resolution scales with w_0^2 the power efficiency scales inversely according to the predictions of Eq. (2) and (3). The drop in conversion efficiency can to some extent be countered by increasing the power in the laser cavity, or by using a crystal with higher non-linearity.

6. Conclusion

In this paper, an all optical technique for efficient upconversion of full 2-dimensional images in one step is demonstrated. Experimentally, 40% power conversion efficiency is demonstrated for upconversion of a 765 nm coherently illuminated object to 488 nm under CW condition. An efficiency which to the author's best knowledge is the highest reported. Further optimization of the enhancement cavity is expected to lead to further increase in the conversion efficiency, or improved resolution.

A simple theoretical description is presented, clarifying the basic nonlinear image formation parameters as well as the limiting factors. The experimental results are in good qualitative as well as quantitative agreement although not all parameters have been included, e.g. the angular acceptance parameter of the crystal.

Generally the presented technique offers the possibility for high-speed upconversion of 2-D images from parts of the spectrum not easily accessed by conventional detectors to e.g. the NIR where simple and efficient Si based image detectors exist.

Acknowledgments

We would especially like to acknowledge Steen Hanson at DTU Fotonik for his valuable help in the mathematical description of the upconversion imaging. This work was supported by the Danish Technical Research Council, grant 274-05-0377.

#116265 - $15.00 USD Received 26 Aug 2009; revised 28 Oct 2009; accepted 28 Oct 2009; published 30 Oct 2009